A DFT and ab Initio Benchmarking Study of Metal−Alkane Interactions and the Activation of Carbon−Hydrogen Bonds

Charity Flener-Lovitt, David E. Woon, Thom H. Dunning, Jr.,* and Gregory S. Girolami*

School of Chemical Sciences, 600 South Mathews Avenue, University of Illinois at Urbana−Champaign, Urbana, Illinois 61801

Received: June 19, 2009; Revised Manuscript Received: November 18, 2009

Density functional theory and ab initio methods have been used to calculate the structures and energies of minima and transition states for the reactions of methane coordinated to a transition metal. The reactions studied are reversible C−H bond activation of the coordinated methane ligand to form a transition metal methyl hydride complex and dissociation of the coordinated methane ligand. The reaction sequence can be summarized as $L_xM(CH_3)H \rightleftarrows L_xM(CH_4) \rightleftarrows L_xM + CH_4$, where L_xM is the osmium-containing fragment $(C_5H_5)Os(R_2PCH_2PR_2)^+$ and R is H or CH_3. Three-center metal−carbon−hydrogen interactions play an important role in this system. Both basis sets and functionals have been benchmarked in this work, including new correlation consistent basis sets for a third transition series element, osmium. Double zeta quality correlation consistent basis sets yield energies close to those from calculations with quadruple-ζ basis sets, with variations that are smaller than the differences between functionals. The energies of important species on the potential energy surface, calculated by using 10 DFT functionals, are compared both to experimental values and to CCSD(T) single point calculations. Kohn−Sham natural bond orbital descriptions are used to understand the differences between functionals. Older functionals favor electrostatic interactions over weak donor−acceptor interactions and, therefore, are not particularly well suited for describing systems—such as σ-complexes—in which the latter are dominant. Newer kinetic and dispersion-corrected functionals such as MPW1K and M05-2X provide significantly better descriptions of the bonding interactions, as judged by their ability to predict energies closer to CCSD(T) values. Kohn−Sham and natural bond orbitals are used to differentiate between bonding descriptions. Our evaluations of these basis sets and DFT functionals lead us to recommend the use of dispersion corrected functionals in conjunction with double-ζ or larger basis sets with polarization functions for calculations involving weak interactions, such as those found in σ-complexes with transition metals.

1. Introduction

The efficient conversion of alkanes into other chemical substances is a highly desirable capability for chemical industry. Alkanes are abundant feedstocks and, therefore, are attractive starting materials for the synthesis of fine chemicals. To develop such syntheses, however, requires the discovery of selective methods to activate particular C−H bonds in alkanes and to replace those hydrogen atoms with other functional groups. Of particular interest is the development of transition metal catalysts to convert alkanes into functionalized derivatives, because such catalysts are often able to promote chemical reactions with high selectivity and high yield. Alkanes, however, interact very weakly with transition metals and their complexes and thus do not readily participate in catalytic cycles under ambient conditions.[1–3]

Alkanes bind weakly to transition metals for several reasons: they are electrically neutral, relatively nonpolarizable, and very poor electron donors and electron acceptors, so that electrostatic, charge transfer, and covalent interactions with metals are weak. Despite these unfavorable attributes, alkanes can bind to transition metal complexes in solution under the right circumstances, and several such complexes are now known.[1,4] These compounds serve as instructive models for the key intermediates in alkane activation reactions, in which carbon−hydrogen bonds are broken. The structural characterization of methane coordination complexes of transition metals is a desirable goal, and the resulting fundamental understandings could assist in the creation of industrially useful catalysts in which alkanes serve as the feedstock.

Most interactions of C−H bonds with metal centers involve weak three-center, two-electron interactions analogous to those in the Dewar−Chatt−Duncanson (DCD) model for the bonding of olefins to transition metals.[5–7] The bonding in such compounds (which are referred to as agostic or σ-complexes) involves σ-donation from a C−H bond into an unoccupied "d" orbital on the metal center, and back-donation from the metal into an unoccupied C−H σ-antibonding orbital. In other cases, the interaction between the metal and the C−H bond is purely electrostatic and involves polarization of the C−H bond by the positively charged metal ion. These latter interactions, which generally are weaker than agostic interactions, have been termed anagostic.[4] Finally, there are examples of what appear from structural data to be σ-interactions but that actually result from delocalization of M−C bonding electrons.[4,8,9]

One of us (G.S.G.) has synthesized a family of cationic osmium complexes $L_xOs(CH_3)(H)^+$, in which a methyl group (CH_3) and a hydride ligand (H) occupy adjacent coordination sites.[10] NMR studies demonstrated that in solution these methyl hydride complexes are in rapid equilibrium with the tautomeric form $L_xOs(CH_4)^+$, in which the metal center is coordinated to a methane molecule formed by joining together the methyl and

* To whom correspondence should be addressed, tdunning@ncsa.uiuc.edu and girolami@scs.illinois.edu.

10.1021/jp9058033
Published on Web 12/31/2009

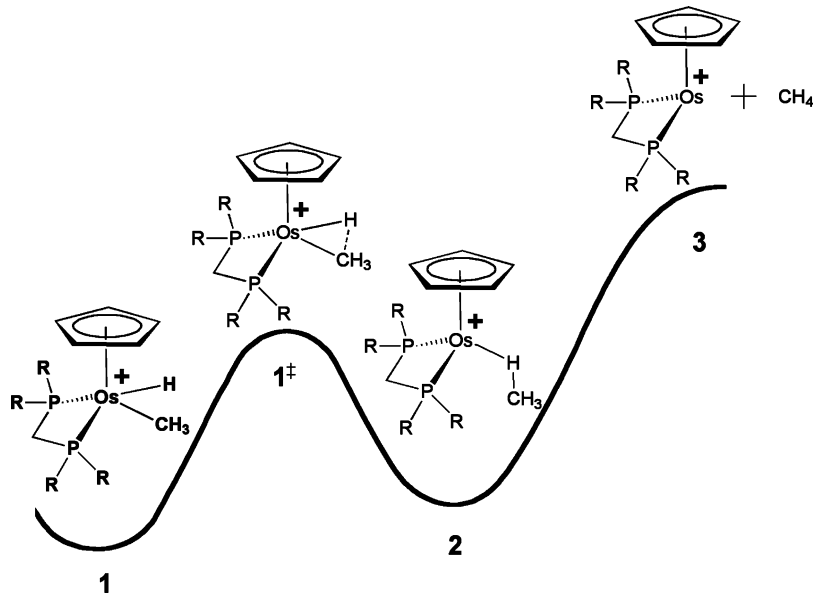

Figure 1. Stationary points on the potential energy surface for methane activation: the methyl hydride complex **1**, the methane coordination complex **2**, and the transition state $\mathbf{1}^{\ddagger}$; R = CH_3 for complexes **1**, **2**, and $\mathbf{1}^{\ddagger}$; R = H for the model complexes **1H**, **2H**, and $\mathbf{1H}^{\ddagger}$. The chemical system **3** (and **3H**) is referred to as the dissociated state in the text.

hydride ligands (Figure 1). The equilibrium between the methyl hydride complex and the methane coordination complex is an example of the reversible activation of methane, and the activation barrier of about 8 kcal mol^{-1} for this process is considerably smaller than the 20−30 kcal mol^{-1} barriers that typically are characteristic of such reactions. This low barrier means that the C−H bond formation and cleavage processes in these osmium complexes are reversible and rapid enough, 100 s^{-1} at −100 °C, to be dynamic on the NMR time scale. The activation energy for loss of the bound methane to generate the dissociated state $L_xOs^+ + CH_4$ was measured to be about 13 kcal mol^{-1}. Again, this is an unusually high dissociation barrier for metal−alkane interactions, rivaled only by those seen in certain rhenium systems.[11,12]

The osmium complexes that have been studied experimentally bear two ancillary ligands: a chelating diphosphine $(CH_3)_2PCH_2P(CH_3)_2$ group and a cyclopentadienyl ring (Figure 1). Interestingly, when the steric and electronic properties of the cyclopentadienyl ring are varied over a large range—$C_5H_x(CH_3)_{5-x}$, where x = 0, 1, 4, and 5—the relative energies of the complexes, and the barriers for the reactions that interconvert them, vary by less than 0.5 kcal mol^{-1}.[13−15]

Two previous computational studies employed the popular B3LYP functional and Pople basis sets to explore the potential energy surface and reaction mechanisms in this osmium system.[16−18] Both Martin and Morokuma supported the conclusions from the experimental study that the methyl hydride complex is in equilibrium with a methane coordination complex and that the transition state for this equilibrium is about 8 kcal mol^{-1} higher in energy than the methyl hydride species. Both authors suggested that changing the cyclopentadienyl ligand from C_5H_5 to C_5Me_5 shifts the total energies of all species on the potential energy surface equally and therefore does not affect the barrier for C–H bond formation and cleavage. This finding is also consistent with the experimental results, as mentioned above.[13−15] The principle purposes of the present study are to explore in more detail now the potential energy surface in this system is affected by (1) changes in the ancillary ligands and (2) changes in the computational method.

For most σ-complex interactions, high-level correlated wave function calculations remain out of reach computationally because the chemical systems are too large, often involving transition metal complexes with 20 atoms or more. Such systems are, however, within the capability of density functional theory (DFT) methods. Few papers have addressed the ability of DFT methods to treat metal−alkane interactions, but generally the results suggest that calculations can provide relatively accurate descriptions of the system[9,22,23] provided that care is taken to choose the correct method.[24−26]

No previous benchmark study has treated σ-complexes of alkenes. Pantazis et al. evaluated the ability of 24 different DFT functionals within a hybrid QM/MM protocol to predict the structure of certain niobium alkyl complexes that exhibit agostic interactions.[8] Of the 24 functionals tested, 11—including the popular B3LYP and MPW1LYP—predicted structures in conflict with experiment. The correlation part of these 11 functionals disobeys the uniform electron gas (UEG) limit, either incorporating the LYP functional or versions of the B97 functionals. These 11 functionals overestimated the strength of donor−acceptor interactions with other π-bonding ligands relative to the agostic interaction. Two LDA functionals, VSXC and SVWN5, correctly predicted the agostic structure but may have done so because these functionals tend to overestimate the correlation energy, which in turn leads to an overestimation of electron delocalization between the C−H and metal orbitals. Eleven other functionals gave reasonable potential energy surfaces, but only six of them correctly predicted the agostic structure to have the minimum energy.

The accuracy of DFT calculations depends mostly on the choice of the functional.[8,27] DFT is inherently an exact method, but the form of the "exact functional" is unknown except for simple systems such as the uniform electron gas.[28] There is no nonempirical way to determine the accuracy of a given functional because there is no systematic basis for improving the functional (at least in the current DFT formalism); there is no parallel to the full configuration interaction limit that allows systematic improvement of wave function based methods. Many different kinds of approximate functionals have been proposed,[28] and their performance for predicting structures and energies varies widely.[29] As with all approximate computational methods, it is essential to benchmark DFT methods against relevant

experimental results or more accurate ab initio methods to determine how well they perform for specific applications.

The goal of the current study is to assess the accuracy and efficiency of various combinations of basis sets and DFT functionals for calculating the energetics of the methane activation reactions of the osmium complexes noted above. The benchmark calculations in the present study are compared against both experimental results and limited high-level coupled cluster calculations of the relevant chemical species (including both minima and transition states). We have investigated popular DFT functionals such as B3LYP, newer dispersion corrected functionals such as Truhlar's M05-2X,[30] and functionals such as MPW1K that were designed to model kinetics.[31] Full optimizations were performed for Hartree−Fock and MP2 ab initio methods and single point energies calculated for coupled cluster with triplet excitations (CCSD(T) and CCSD). We also evaluated the electronic structure of the relevant species in terms of the Kohn−Sham[32] and natural bond orbital[33] representations, in order to determine how effectively the different functionals describe the σ-complex interaction.

The findings of the present study are potentially relevant to all chemical phenomena that involve weak interactions, and not just those responsible for the activation of C−H bonds. Previous benchmarking studies have largely dealt with small molecules; the current paper is noteworthy because it is one of the first to benchmark the ability of different DFT methods to deal with weakly bonded complexes of transition metals and the first to test the performance of the new correlation consistent basis sets that have recently been developed for late transition metals by Peterson and co-workers.[34]

2. Methods

Geometries were optimized using Gaussian03 Rev. D.01 and E.01[35] (M05-2X functional only) without any constraints. The crystal structure of $(C_5Me_5)Os(Me_2PCH_2PMe_2)(H)$ was used as a starting point for structure optimizations.[14] Two different complexes were studied, the experimentally known $[(C_5H_5)Os(Me_2PCH_2PMe_2)(H)CH_3)]^+$, **1**,[15] and the model complex $[(C_5H_5)Os(H_2PCH_2PH_2)(H)(CH_3)]^+$, **1H**. For each complex, three points on the potential energy surface were characterized: the methyl hydride complex (**1** and **1H**), the methane coordination complex (**2** and **2H**), and the transition state (**1**‡ and **1H**‡) between them. In some cases, the energy of the dissociated state $[(C_5H_5)Os(R_2PCH_2PR_2)]^+ + CH_4$ (**3** and **3H**) was also calculated; the energy of this state with respect to **2** or **2H** affords a measure of the methane binding energy. In these latter calculations, the structure of the fragment $[(C_5H_5)Os(R_2PCH_2PR_2)]^+$ was allowed to relax. Owing to the flatness of the potential energy surface, all stationary points were determined using the GDIIS method and internal options to decrease step size. The transition states connecting the methyl hydride complex with the methane coordination complex were determined from optimizations using redundant internal coordinates. Frequency calculations were performed to confirm that optimized minima and transition states were true stationary points. For the latter, imaginary frequencies with a magnitude less than 25 cm^{-1} were considered to be close enough to 0 that they could be safely ignored. Intrinsic reaction coordinate (IRC) calculations were used to confirm the transition state geometry.

The benchmark calculations for the basis sets were performed with the B3LYP functional. All molecules were fully optimized for each basis set, and zero point energies were computed for each molecule. The impact of basis set superposition error (BSSE) is expected to be small for these complexes when studied by DFT.[36,37] Counterpoise corrections were performed for selected methods and basis sets:[38] the corrections were small (<0.2 kcal mol^{-1}) and affected all species on the potential energy surface nearly equally, confirming that the effect of BSSE is minimal (the BSSEs are small and cancellation makes the net impact even smaller).

TABLE 1: DFT Methods Studied

method	method type	% HF exchange	exchange functional	correlation functional
BMK	HMGGA	42	BMK	BMK
B3LYP	HGGA	20	becke88	Lee−Yang−Parr
BB1K	HMGGA	42	becke88	becke95
MPW1k	HGGA	42.8	mod PW91	PW91
PBE0	HGGA	25	Perdew−Burke−Ernzerhof	
M05−2X	HMGGA	56	m05-2x	
TPSSh	HMGGA	10	Tao−Perdew−Staroverov−Scuseria	
BP86	GGA	0	becke88	perdew86
PBE	GGA	0	Perdew−Burke−Ernzerhof	
SVWN5	LSDA	0	LSA	VWN5

Structures were fully optimized for ten DFT methods. We tested one local spin density approximation (LSDA) functional (SVWN5),[39,40] two pure gradient corrected (GGA) functionals (BP86,[41,42] and PBE[43]), three hybrid GGA (HGGA) functionals (B3LYP,[41,42,44] MPW1K,[31,43,45,46] and PBE0[43]), and four hybrid meta-GGA (HMGGA) functionals (TPSSH,[47] BB1K,[41,44,48] BMK,[49] and M05-2X[50]). All benchmark comparisons for the DFT methods employed basis set combination cc10 (see Table 3). The density functional methods tested are listed in Table 1. Details about the various functionals can be found in the cited references. Keywords and IOP commands for functionals are listed in the Supporting Information. NBO analyses for each method were performed on the methane coordination complex **2H** with NBO 3.0;[51] NBO options included searching for delocalized orbitals (RESONANCE) and three-center bonds (3CBOND).

For the ab initio methods, the structures of **1H**, **1H**‡, **2H**, and **3H** were fully optimized with MP2 and HF. Single point energy calculations were performed using the CCSD and CCSD(T) methods at optimized B3LYP, M05-2X, and MP2 geometries. SCF energies are reported for all MP2, CCSD, and CCSD(T) structures.

3. Results and Discussion

The results are divided into five sections. In the first section, we summarize how optimized geometric parameters vary with different methods and basis sets. In the second section, we benchmark basis sets for a fixed method (B3LYP), and in the third section, we benchmark the behavior of the functionals for a fixed basis set combination (cc10). In the fourth section, orbital analysis is used to gain insights into the results from the various functionals. In the last section, we discuss single point energies calculated from ab initio methods and compare them with the corresponding DFT energies.

Geometries of Stationary Points. Structures of the methyl hydride complex **1**, the transition state **1**‡, and the methane coordination complex **2**, as well as the model complexes **1H**, **1H**‡, and **2H**, have been optimized for the combinations of functionals shown in the (see Figure 1 for schematic drawings of these structures). The ranges of bond lengths, bond angles, and tilt angles[52] found for **1**, **1**‡, and **2** are shown in Table 2; a selection of key structural parameters for each basis set is available in the Supporting Information. For all methods and combinations of basis sets, the optimized geometries of **1**

TABLE 2: Sample Geometric Parameters of the Simplified Phosphine Complexes

parameter	methyl hydride (**1H**)	transition state (**1H**‡)	methane complex (**2H**)
Os−H (Å)	1.59−1.62	1.61−1.66	1.85−1.91
Os−C (Å)	2.20−2.24	2.26−2.33	2.55−2.68
C−H (Å)	2.13−2.17	1.45−1.50	1.14−1.17
H−Os−C (deg)	66.7−67.4	39.0−41.4	21.4−24.8
tilt angle (deg)	49.3−50.6	51.5−52.5	51.1−51.8

and **2** have much in common, and the positions of the ancillary ligands are similar to those seen in the crystal structure of a related compound, the osmium hydride $(C_5Me_5)Os(Me_2PCH_2PMe_2)H$.[14]

For the methyl hydride complex **1**, the calculated Os−H bond distance varies from 1.59 to 1.62 Å, depending on the computational method used. Similarly, the calculated Os−CH_3 bond distance varies from 2.20 to 2.24 Å, and the calculated nonbonded C···H contact distance between the Os−CH_3 and Os−H groups varies from 2.13 to 2.17 Å. For the methane coordination complex **2**, the bond lengths change in the expected fashion: the Os−H and Os−C(CH_3) distances lengthen considerably, and the C···H contact distance between the former Os−CH_3 and Os−H groups approaches the 1.09 Å distance seen for free methane.[53] Relative to the variations in the distances calculated for **1**, however, the corresponding distances in **2** show somewhat larger variations depending on the computational method employed. Thus, the calculated Os−H distance varies from 1.85 to 1.91 Å, the calculated Os−C(CH_3) distance varies from 2.55 to 2.68 Å, and the C−H distance between the former Os−CH_3 and Os−H groups varies from 1.14 to 1.17 Å. The larger variations reflect the shallowness of the potential energy surface near this stationary point, which in turn results from the weakness of the Os−methane σ-interaction. No clear correlation could be found between these variations and nature of the calculational method used.

The geometry of the transition state **1**‡ that connects **1** and **2** also varies widely depending on the computational method employed. Thus, the Os−H distance ranges from 1.47 to 1.51 Å, the Os−C(CH_3) distance varies from 2.26 to 2.33 Å, and the incipient C···H bond between the hydride and methyl group ranges in length from 1.45 to 1.50 Å. Because the calculated structures of the methane coordination complex **2** and the transition state **1**‡ depend most strongly on the computational method, it is not surprising that the calculated energies of these species are also most sensitive to the method employed, as will be discussed below.

Dependence of B3LYP Energies on Choice of Basis Set. For the osmium system described above, we carried out an extensive investigation of how different basis sets affect the potential energy surface calculated with the popular B3LYP functional.[42,54] Table 3 lists the 22 basis sets studied along with the total number of basis functions used for each complex and the energies of stationary points on the potential energy surface with respect to the methyl hydride complex. Pople style basis sets were used to analyze the experimentally studied system (**1**, **2**, and the transition state **1**‡), whereas correlation consistent basis sets were used to analyze the simplified phosphine system (**1H**, **2H**, and the transition state **1H**‡). Pople basis sets are given symbols beginning with the letter "p", whereas correlation consistent basis sets are given symbols beginning with the letters "cc". Results of this study are summarized below; additional discussion of the basis set variations can be found in the Supporting Information.

Figures 2 and 3 show calculated energies of the transition state **1**‡ and methane complex **2** relative to the methyl hydride complex **1** for all basis sets tested. Calculations with the Pople basis sets predict that the transition state **1**‡ lies 5.5−8.0 kcal mol^{-1} higher in energy than **1** and that the methane coordination complex **2** lies 0.0−2.8 kcal mol^{-1} higher than **1** (Figure 2). For comparison, the experimental free energy of **1**‡ is 8.1 kcal mol^{-1} at −100 °C in solution. The calculated energies of the stationary points and transition states vary over a range of about 2.5 kcal mol^{-1}, depending, for example, on whether double-ζ or triple-ζ Pople basis sets are used on Os and CH_4. This variation is large in the context of weak interactions such as those in the present system, because the energy differences of interest (e.g., between **1** and **2**) are of the same order. What this means is that, for weak interactions involving hydrogen atoms, a significant loss of computational accuracy results from attempts to save on computational costs by reducing the size of the Pople basis set, in particular changing the description of the Os−CH_4 atoms from triple-ζ to double-ζ.[48]

Correlation consistent basis sets are excellent choices for benchmarking studies because they can be extended to approach the complete basis set limit as closely as desired (within the constraint of computational feasibility).[55–57] The structures of **1H** and **2H** and the corresponding transition state **1H**‡ (all bearing the simplified phosphine) were optimized using 11 different combinations of the correlation consistent basis sets, and the energy of each optimized structure was calculated (Table 3 and Figure 3). These energies are compared to the single point energies calculated for the most complete basis set, in which quadruple-ζ quality sets were used on all atoms (cc11 in Table 3). For this latter basis set, the energy of the methane coordination complex **2H** relative to methyl hydride **1H** is −0.58 kcal mol^{-1}, whereas the energy of the transition state that connects these two structures is 4.62 kcal mol^{-1}.[58] The variations in the energies of the simplified phosphine complexes **1H**‡ and **2H** relative to **1H** computed with different correlation consistent basis sets is only 0.7 kcal mol^{-1}. We find that using even relatively small double-ζ quality correlation consistent basis sets for the Os−CH_4 atoms produce results within 0.4 kcal mol^{-1} of those obtained with much larger quadruple-ζ quality sets (Figure 3). In addition, calculations with a triple-ζ basis set for the Os−CH_4 atoms (4.98 and −0.57 kcal mol^{-1} for **1**‡ and **2**, respectively) are less than 0.3 kcal different from extrapolations to the estimated complete basis set limit (5.06 and −0.21 kcal mol^{-1} for **1**‡ and **2**, respectively).

If we assume that the results above for the B3LYP functional are representative, these calculations suggest that both Pople and correlation consistent basis sets are suitable for treating late transition metal σ-complexes, provided sufficiently large basis sets (double-ζ with polarization functions, or better) are used for the Os−CH_4 atoms. One difference is that the Pople basis sets give energies for the methane complexes that are 1−2 kcal mol^{-1} lower (relative to the methyl hydride species) than the energies calculated from the correlation consistent basis sets. We hesitate to speculate on the reasons for the differences in energies calculated using the Pople and Dunning basis sets, but it is well appreciated that these basis sets often give small but systematically different results in many systems.[59,60]

Dependence of DFT Energies on Choice of Functional. To determine which functionals are best able to describe the bonding in σ-complexes accurately, we used 10 different DFT functionals and the cc10 basis set combination to calculate stationary points on the reaction path for the system in which the osmium bears the simplified phosphine ligand (**1H**, **1H**‡,

TABLE 3: Zero-Point Corrected Energies Relative to Os−CH_3H (1 and 1H) for All Basis Sets Studied Using the B3LYP Functional

				no. of basis functions		energies[a]		energies[b]	
label	metal	CH_4	other atoms	**1**	**1H**	**1‡**	**2**	**1H‡**	**2H**
p1	lanl2dz	6-31G(d)	6-31G(d)	258		7.55	2.11		
p2	lanl2dz	6-31G(d′)	6-31G(d′)	258		7.26	0.02		
p3	lanl2dz	6-311G(d)	6-311G(d)	276		7.96	2.82		
p4	sdd	6-31G(d)	6-31G(d)	272		6.77	0.85		
p5	sdd	6-31G(d′)	6-31G(d′)	272	200	6.42	0.53	4.61	−1.60
p6	sdd_polarized	6-31G(d′)	6-31G(d′)	279		6.63	0.80		
p7	sdd_polarized	6-31+G(d)	6-31+G(d)	331		6.78	0.87		
p8	sdd_polarized	6-31+G(d,p)	6-31G(d)	295	223	7.93	1.06	4.50	−1.52
p9	sdd_polarized	6-31+G(d,p)	6-31+G(d,p)	400	288	5.88	0.82	4.40	−1.72
p10	sdd_polarized	6-311+G(d,p)	6-31G(d)	303		5.86	1.09		
p11	sdd	cc-pvDZ	cc-pvDZ	341		5.49	0.89		
cc1	cc-pVDZ-PP	cc-pVDZ	cc-pVDZ		247			4.57	−0.54
cc2	cc-pVTZ-PP	cc-pVDZ	cc-pVDZ		272			4.82	−0.10
cc3	cc-pwCVDZ-PP	cc-pVDZ	cc-pVDZ		263			4.65	−0.24
cc4	cc-pwCVTZ-PP	cc-pVDZ	cc-pVDZ		306			4.83	0.08
cc5	cc-pwCVTZ-PP	aug-cc-pVDZ	aug-cc-pVDZ		447			4.81	−0.01
cc6	cc-pVQZ-PP	cc-pVTZ	cc-pVTZ		587			4.98	−0.42
cc7	cc-pVDZ-PP	aug-cc-pVTZ	cc-pVTZ		288			4.77	0.11
cc8	cc-pVTZ-PP	cc-pVTZ	cc-pVDZ		324			4.98	−0.57
cc9	aug-cc-pVTZ-PP	aug-cc-pVTZ	cc-pVDZ		401			4.94	−0.41
cc10	cc-pVTZ-PP	trunc-cc-pVTZ	cc-pVDZ	393	297	6.64	2.84	5.05	−0.60
cc11	cc-pVQZ-PP	cc-pVQZ-PP	cc-pVQZ-PP		1052			4.62	−0.58
cc12	cc-pVQZ-PP	cc-pVQZ	cc-pVDZ		449			5.05	−0.38
complete basis set limit								**5.06**	**−0.213**
experimental						**8.1**			

[a] In kcal mol^{-1} relative to **1**. [b] In kcal mol^{-1} relative to **1H**. [c] Single point energy calculation with zero point correction from cc10.

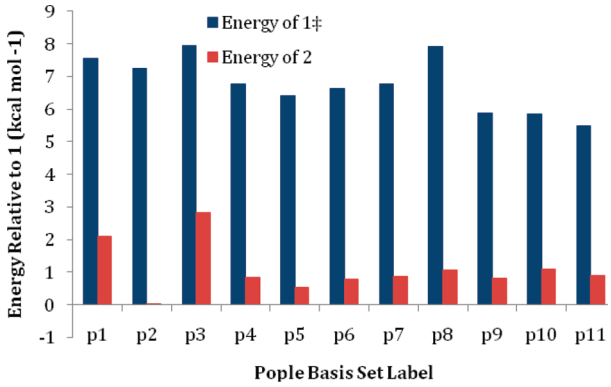

Figure 2. Variation in energy (kcal/mol) of the transition state **1‡** (blue) and of the methane coordination complex **2** (red) with respect to the methyl/hydride complex **1**, using Pople basis sets.

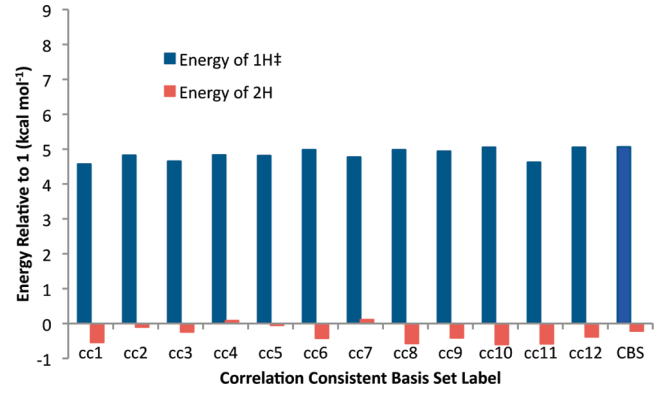

Figure 3. Variation in energy (kcal/mol) of the transition state **1H‡** (blue) and of the methane coordination complex **2H** (red) with respect to the methyl/hydride **1H**, using correlation consistent basis sets.

2H). The energies of **1H‡** and **2H** relative to complex **1H** are shown in Figure 4. Values for the zero point corrected energies for the transition state **1H‡** and methane complex **2H** relative to the methyl hydride **1H** along with the zero point and Gibbs free energies for each species can be found in the Supporting Information.

The variation in the relative energy of the transition state **1H‡** is ± 2 kcal mol^{-1}, ranging from a low of 3.67 kcal mol^{-1} for BMK to a high of 5.55 kcal mol^{-1} for TPSSh. Interestingly, all of these values are all smaller than the 7.9 kcal mol^{-1} obtained from single point calculations with the CCSD(T) ab initio correlated method (*see below*). This result is not surprising because DFT systematically underestimates transition state energies.[46,48] What is surprising, however, is that transition state energies obtained from the selected "fourth rung" HMGGA functionals[61] vary more than the barriers calculated using the first and second rung LSDA and GGA functionals. In the HMGGA functionals employed here, the kinetic energy density is used to provide a density functional approximation to delocalized electron exchange and an improved description of electron correlation, both of which have been proposed to be important for dispersion type interactions.[30,62] It is known that an inaccurate description of the kinetic energy density leads to the underestimation of transition state energies.[63,64]

Of all the stationary points on the potential energy surface in the present system, the relative energy of the methane complex **2H** is most strongly dependent on the choice of DFT functional (Figure 4). In contrast to the Pantazis benchmark study of niobium σ-complexes,[8] all functionals in the present study found the osmium σ-complex **2H** to be a minimum on the potential energy surface. The relative energy of **2H** varies from a low of −1.93 kcal mol^{-1} for BMK to a high of +4.33 kcal mol^{-1} for the LSDA functional SVWN5. Hartree−Fock based methods (see below) afford the lowest relative energy for **2H**. The pure DFT methods BP86, PBE, and LSDA calculate

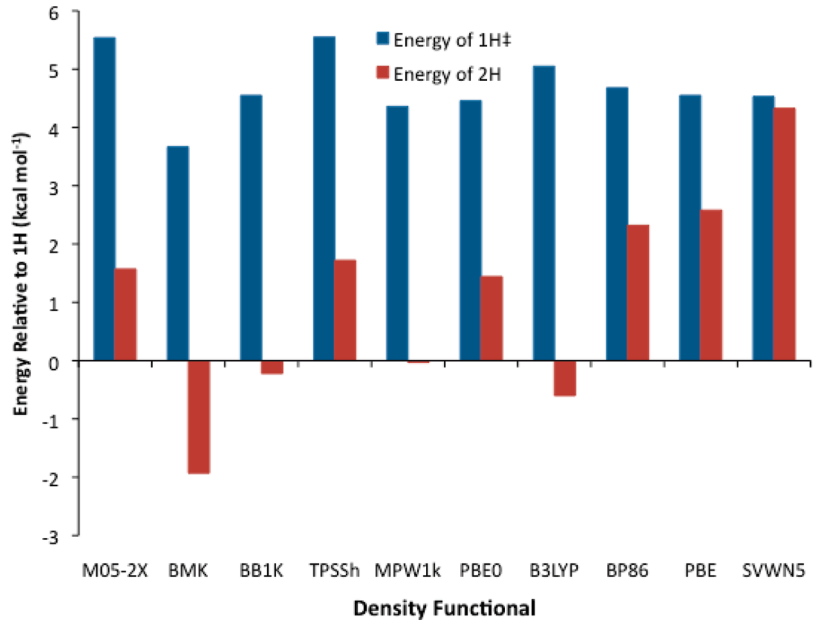

Figure 4. Variation in energy (kcal/mol) of the transition state **1H**‡ (blue) and of the methane coordination complex **2H** (red) relative to the methyl/hydride **1H**, using various DFT functionals and the cc10 basis set.

the highest energies for **2H**, perhaps due to the lack of Hartree−Fock exchange. This result suggests that pure DFT methods overestimate electron correlation between the osmium and phosphine at the expense of the weakly bonded methane. Even though all of the functionals found that **2H** was a local minimum, the large variation in calculated energies suggests that the functionals treat the bonding in this σ-complex rather differently. We will explore details of the bonding in the next section.

Frontier Orbital Analyses. To better understand how well the different functionals describe the bonding in the σ-complex, we compared the Kohn−Sham (KS)[32] and natural atomic orbitals (NAO)[33] for the methane coordination complex **2H**. KS orbitals are derived naturally from the coefficients of the eigenfunctions generated in the DFT calculations. They are an improvement over the nonelectron correlated Hartree−Fock orbitals and have been used as tools for qualitative MO descriptions.[28] We find that, to first order, the KS HOMOs for the osmium complexes are essentially identical irrespective of the functional chosen. The HOMO for the methane complex **2H** is highly delocalized over the entire molecule (Figure 5) but includes a bonding interaction between the osmium atom and the C−H σ-orbitals. The delocalized nature of the HOMO suggests that the nature of the osmium−methane interaction (and the energy of **2H** relative to the methyl hydride complex **1H**) should be influenced by the choice of the ancillary cyclopentadienyl and phosphine ligands.

In contrast, natural atomic orbitals (NAOs) are derived from the diagonal of the one electron density matrix.[33] Natural bond order analysis combines the NAOs to form natural bond orbitals (NBOs). As a result, NBOs are highly sensitive to the post hoc densities generated by the DFT calculations and, therefore, should reveal differences in how different functionals describe the σ-complex interaction.[8,9,22] NBOs have been used in the past to determine if a molecule exhibits σ-complex interactions,[65] but in this case, we use NBOs to highlight differences between functionals. A summary of important data is shown in Table 4. For all 10 functionals tested, the NBO analysis shows that there are three-center bonds between the metal and the carbon atoms in the cyclopentadienyl ring. However, only five of the

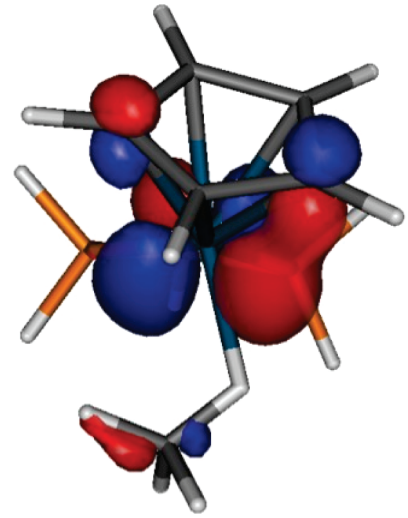

Figure 5. Depiction of the delocalized Kohn−Sham HOMO for **2H** showing the mixing between the "d" orbital on osmium and C−H σ-orbital on methane. The orbital shown comes from M05-2X calculations; the isovalue is 0.0767 e Å^{-3}. Qualitatively, the HOMO was identical for all functionals.

functionals studied—M05-2X, BMK, BB1K, MPW1K, and SVWN5—yielded NBOs for the methane complex **2H** that include a three-center bond between the osmium and the coordinated methane ligand. Of these five functionals, all include kinetic parameters except SVWN5. NBOs calculated from PBE0 do not show a three-center bond with the methane ligand, which contradicts other studies that suggested that PBE0 is useful for describing σ-complex interactions.[66,67] We conclude that PBE0 and TPSSh, along with pure GGA functionals such as BP86 and PBE, are not satisfactory choices to study molecules with weak donor−acceptor interactions such as those in the present study.

We have analyzed several functionals in greater detail. One of the oldest functionals (SVWN5) seems to outperform some functionals developed later. Of all of the functions that do not explicitly account for kinetic energy density, only SVWN5 identifies a three-center NBO with the methane ligand. This

TABLE 4: NBO Data Including Natural Charges and Three-Center Two-Electron Bonding Orbital Information for Os, C, and H Atoms Potentially Involved in Three-Center Bonding

	natural charge				
method	Os	H (on Os)	C (CH_3)	3c2e bond?	obeys UEG?[a]
M052X	−0.94649	0.23341	−0.73884	yes	yes
BMK	−0.77582	0.22758	−0.73073	yes	no
BB1K	−0.98959	0.23757	−0.72419	yes	yes
TPSSh	−0.94386	0.22038	−0.68015	no	yes
MPW1k	−0.99505	0.23585	−0.71412	yes	yes
PBE0	−0.99742	0.24587	−0.73538	no	yes
B3LYP	−0.16897	0.24636	−0.74972	no	no
BP86	−0.92760	0.23920	−0.73264	no	yes
PBE	−0.95577	0.24872	−0.75237	no	yes
SVWN5	−1.07764	0.29616	−0.82659	yes	yes
HF	0.04922	0.21999	−0.66355	no	

[a] UEG = uniform electron gas limit.

finding is probably related to the tendency of SVWN5 to overestimate binding between atoms in molecules due to an exchange hole effect.[28,68] This effect is expressed in the large magnitude of the natural charges on osmium and the carbon atom of the coordinated methane ligand (−1.08 and −0.83, respectively). These natural charges, which are larger in magnitude than those generated from any of the other DFT functionals, illustrate that when the SVWN5 functional is used electron density moves freely between atoms in a molecule. This conclusion is not surprising because SVWN5 is used primarily for modeling electrons in metallic phases.[40]

B3LYP is known to overestimate electron correlation between atoms in a molecule due to violations of the UEG limit that cause the description to lack the "free-electron-like" character necessary to describe weak interactions.[69] Consequently, this functional does a poor job of describing the osmium−methane σ-complex interaction. For the methane complex **2H**, the natural charges of the osmium atom (−0.17), the methane carbon atom (−0.75), and the hydrogen atom bridging between osmium and this carbon (0.25), as calculated by B3LYP, are relatively small. More importantly, no three-center bond between osmium and methane is found by NBO analysis of the B3LYP orbitals.

Of all the functionals tested, only one specifically addresses the issue of dispersion interactions in weakly bound complexes, Truhlar's M05-2X functional. Previous studies have shown that M05-2X, which produces results consistent with more computationally expensive ab initio methods such as CCSD(T) and CASPT2, performs well for molecules such as π-complexes and proteins that contain dispersion-like interactions.[50,70–72] Our results suggest that M05-2X may describe σ-complex interactions as accurately as correlated methods, but for a fraction of the cost. It is likely that other dispersion corrected functionals, such as Grimme's PBE-D, may also offer accurate descriptions of σ-complexes.[73]

As noted in the introduction, Pantazis et al. concluded that the correlation contribution of a density functional should obey the uniform electron gas limit if the functional is to describe correctly the balance between σ-complex interactions and competing M−X π interactions.[8] Two of the functionals we studied, B3LYP and BMK, violate this limit. Although NBO analysis of B3LYP fails to identify the osmium−methane interaction, BMK performs surprising well considering that in other systems it affords large errors for metal−atom binding interactions.[48] We surmise that BMK includes too much uncorrected Hartree−Fock exchange, which causes this functional to overestimate the strength of the osmium−methane interaction. Even though NBO analysis of the BMK wave functions identifies the presence of a three-center interaction with the coordinated methane ligand, this result is most likely a consequence of error cancellation rather than functional accuracy. Thus, we do not recommend BMK for studies of molecules with weak interactions.

The remaining functionals are unsuited for studying σ-complex complexes, because analysis of the wave functions did not find three-center NBOs with the methane ligand. Instead, we recommend that the functionals M05-2X and MPW1K are best suited for analyzing weak interactions such as the σ-complexes in the present study.

TABLE 5: Single Point Energies in kcal mol^{-1} of the Transition State 1H‡, the Methane Coordination Complex 2H, and the Dissociated Methane State 3H, Relative to the Methyl/Hydride 1H from ab Initio Methods Calculated from DFT Optimized Structures

method	1H‡	2H	3H
HF	4.9	−12.7	−10.0
MP2		8.7	9.5
ccsd//MP2b		2.7	18.9
ccsd(t)//MP2b		4.5	23.0
M05-2X	5.5	1.6	15.9
ccsd//m05-2xb	7.6	0.9	15.9
ccsd(t)//m05-2xb	8.0	3.1	26.9
B3LYP	5.1	−0.6	7.0
CCSD//B3LYPb	7.5	0.8	22.6
CCSD(T)//B3LYPb	9.7	3.4	27

[a] Full optimization and frequency. [b] Nonzero point corrected energies.

Ab Initio Methods. Due to the size of the complexes investigated in this work, and the present limitations in computational speed, calculations with correlated ab initio methods beyond MP2 were restricted to single point energies. In addition to calculating optimized HF and MP2 structures and frequencies, we also calculated CCSD and CCSD(T) single point energies for the methyl hydride complex **1H**, the methane coordination complex **2H**, and the transition state **1H**‡ at B3LYP, M05-2X, and MP2 geometries using the cc10 basis set. The energies relative to **1H** are shown in Table 5; the absolute energies can be found in the Supporting Information.

Hartree−Fock results show that the energy of the transition state **1H**‡ is reasonable (4.9 kcal mol^{-1}) but, unlike the results for other ab initio methods, the energy of **3H** is calculated to be lower than that of **1H**. In the MP2 calculations, no structure for the transition state **1H**‡ was located, and the methane coordination complex **2H** is calculated to be a barely bound minimum 8.7 kcal mol^{-1} higher in energy than the methyl hydride **1H**, a finding that is far out of line with all of the other results (Table 5). A possible explanation for our inability to locate the transition state with MP2 is that the bond energies it calculates for transition metal complexes are known to suffer from errors as large as 30 kcal mol^{-1} due in part to large basis set superposition errors.[36,74] Another contributor to this error is the inadequacy of perturbation theory in describing strong electron correlation.[75] Likewise, the calculated CCSD and CCSD(T) energies from MP2 geometries are in poor agreement with MP2 energies. The energy of **2H** is 8.7 kcal mol^{-1} for MP2 but 2.7 and 4.5 kcal mol^{-1} for CCSD and CCSD(T), respectively. The energy of **3H** is 9.5 kcal mol^{-1} for MP2, whereas it is 18.9 and 23.0 kcal mol^{-1} for CCSD and CCSD(T), respectively. This poor agreement between coupled cluster and

perturbation energies suggests that MP2 should not be used to model this class of molecules.

In contrast, the calculated single point energies from M0-2X and B3LYP optimized structures are in good agreement with the CCSD and CCSD(T) single point energies. For example, the calculated energy of the transition state $\mathbf{1H}^{\ddagger}$ of 5.5 kcal mol^{-1} from M05-2X compares well with the equilibrium (noncorrected) energies of $\mathbf{1H}^{\ddagger}$ of 7.6 and 8.0 kcal mol^{-1} for CCSD and CCSD(T), respectively. Likewise, M05-2X predicts that the methane coordination complex **2H** is 1.6 kcal mol^{-1} higher in energy than the methyl/hydride **1H**, vs the CCSD and CCSD(T) values of 0.9 and 3.1 kcal mol^{-1}. The relative energy for the dissociated state **3H** was identical for M05-2X and CCSD (15.9 kcal mol^{-1}) whereas the CCSD(T) value was much higher (26.9 kcal mol^{-1}). The B3LYP energies are also in good agreement with CCSD and CCSD(T) energies calculated for B3LYP optimized geometries.

4. Conclusions

This study characterizes how the choice of basis sets *and* functionals affects the ability of DFT methods to predict the geometries and energies of σ-complex interactions in transition metal complexes. Both Pople and correlation consistent basis sets are suitable for treating such weak interactions, provided that sufficiently large basis sets (double-ζ with polarization functions, or better) are used on the Os$-$CH$_4$ atoms involved in the σ-complex interaction. We show that cc-pVTZ basis sets on the atoms of importance (the metal and the interacting alkane molecule) and cc-pVDZ on other atoms provide results as good as those from the larger cc-pVQZ basis sets. Different DFT methods produce very similar potential energy surfaces, but the popular B3LYP functional systematically underestimates the energies of molecules characterized by weak interactions, such as the alkane coordination complexes in the present study. For all of the methods, the Kohn$-$Sham HOMO for the methane species **2** is a three-center bond between osmium and the carbon and hydrogen atoms of the coordinated methane ligand. However, natural bond order analysis shows that only five of the functionals (not including the popular B3LYP) correctly predict the presence of a three-center interaction between osmium and methane. Dispersion corrected functionals such as Truhlar's new M05-2X functional yield energies close to CCSD(T) results and also correctly predict the presence of a covalent σ-complex interaction in the complexes. Dispersion corrected functionals used with polarized triple-ζ basis sets or their equivalent are recommended for studies of weak metal σ-complexes.

Acknowledgment. The authors thank Professor Kirk Peterson for use of the new correlation consistent basis sets for Os and Professor Gernot Frenking for advice on density functionals. This research was supported in part by the National Science Foundation through TeraGrid resources provided by the National Center for Supercomputing Applications and through Grant CHE07-50422 to G.S.G. Additionally, C.F.-L. would like to acknowledge the support of the German$-$American Fulbright Commission and the Central European Summer Research Institute.

Supporting Information Available: Tables S1$-$S6 contain equilibrium point energies and geometrical parameters obtained from all basis set combinations and DFT methods. This material is available free of charge via the Internet at http://pubs.acs.org.

References and Notes

(1) Chen, G. S.; Labinger, J. A.; Bercaw, J. E. *Proc. Natl. Acad. Sci. U.S.A.* **2007**, *104*, 6915–6920.
(2) Bergman, R. G. *Science* **1984**, *223*, 902–908.
(3) Kubas, G. *Proc. Natl. Acad. Sci. U.S.A.* **2007**, *104*, 6901–6907.
(4) Brookhart, M.; Green, M. L. H.; Parkin, G. *Proc. Natl. Acad. Sci. U.S.A.* **2007**, *104*, 6908–6914.
(5) Frenking, G. *J. Organomet. Chem.* **2001**, *635*, 9–23.
(6) Kubas, G. J. *J. Organomet. Chem.* **2001**, *635*, 37–68.
(7) Mingos, D. M. P. *J. Organomet. Chem.* **2001**, *635*, 1–8.
(8) Pantazis, D. A.; McGrady, J. E.; Maseras, F.; Etienne, M. *J. Chem. Theory Comput.* **2007**, *3*, 1329–1336.
(9) Pantazis, D. A.; McGrady, J. E.; Besora, M.; Maseras, F.; Etienne, M. *Organometallics* **2008**, *27*, 1128–1134.
(10) Gross, C. L.; Girolami, G. S. *J. Am. Chem. Soc.* **1998**, *120*, 6605–6606.
(11) Lawes, D. J.; Darwish, T. A.; Clark, T.; Harper, J. B.; Ball, G. E. *Angew. Chem., Int. Ed.* **2006**, *45*, 4486–4490.
(12) Lawes, D. J.; Geftakis, S.; Ball, G. E. *J. Am. Chem. Soc.* **2005**, *127*, 4134–4135.
(13) Dickinson, P. PhD Thesis, University of Illinois at Urbana-Champaign, 2006.
(14) Gross, C. L. PhD Thesis, University of Illinois at Urbana-Champaign, 1997.
(15) Jew, R. L. PhD Thesis, University of Illinois at Urbana-Champaign, 2008.
(16) Szilagyi, R. K.; Musaev, D. G.; Morokuma, K. *Organometallics* **2002**, *21*, 555–564.
(17) Martin, R. L. *J. Am. Chem. Soc.* **1999**, *121*, 9459–9460.
(18) Both methods used Pople Basis sets of 6-31+G(p) quality and contractions of the Los Alamos effective core potential and double zeta valence descriptions.
(19) Carreun-Macedo, J.-L.; Harvey, J. N.; Poli, R. *Eur. J. Inorg. Chem.* **2005**, 2999–3008.
(20) Khaliullin, R. Z.; Cobar, E. A.; Lochan, R. C.; Bell, A. T.; Head-Gordon, M. *J. Phys. Chem. A* **2007**, *111*, 8753–8765.
(21) Janak, K. E.; Churchill, D. G.; Parkin, G. *Chem. Commun.* **2003**, 22–23.
(22) Etienne, M.; McGrady, J. E.; Maseras, F. *Coord. Chem. Rev.* **2009**, *253*, 635–646.
(23) Vastine, B. A.; Webster, C. E.; Hall, M. B. *J. Chem. Theory Comput.* **2007**, *3*, 2268–2281.
(24) Cobar, E.; Khaliullin, R.; Bergman, R. G.; Head-Gordon, M. *Proc. Natl. Acad. Sci. U.S.A.* **2007**, *104*, 6963–6968.
(25) Eisenstein, O.; Jean, Y. *J. Am. Chem. Soc.* **1985**, *107*, 1177–1186.
(26) Clot, E.; Eisenstein, O. In *Principles and Applications of Density Functional Theory in Inorganic Chemistry II*; Kaltsoyannis, N., McCrady, J. E., Mingos, D. M. P., Eds.; Springer: Berlin/Heidelberg, 2004; Vol. 113, p 1-2-36.
(27) Sousa, S. F.; Fernandes, P. A.; Ramos, M. J. *J. Phys. Chem. A* **2007**, *111*, 10439–10452.
(28) Koch, W.; Holthausen, M. C. *A Chemist's Guide to Density Functional Theory*, 2nd ed.; Wiley-VCH: Weinheim, 2001.
(29) Wilson, E. K. *Chem. Eng. News* **2008**, *86* (26), 34–37.
(30) Schultz, N. E.; Zhao, Y.; Truhlar, D. G. *J. Phys. Chem. A* **2005**, *109*, 11127–11143.
(31) Lynch, B. J.; Fast, P. L.; Harris, M.; Truhlar, D. G. *J. Phys. Chem. A* **2000**, *104*, 4811–4815.
(32) Kohn, W.; Sham, L. J. *Phys. Rev.* **1965**, *140*, A1133.
(33) Reed, A. E.; Weinstock, R. B.; Weinhold, F. *J. Chem. Phys.* **1985**, *83*, 735–746.
(34) Figgen, D.; Peterson, K. A.; Dolg, M.; Stoll, H. *J. Chem. Phys.* **2009**, *130*, 164108–12.
(35) Frisch, M. J.; et al. *Gaussian03, Rev. D.01 and E.01*; Gaussian, Inc.: Wallingford, CT, 2004.
(36) de Jong, G. T.; Sola, M.; Visscher, L.; Bickelhaupt, F. M. *J. Chem. Phys.* **2004**, *121*, 9982–9992.
(37) Zaric, S.; Hall, M. B. *J. Phys. Chem. A* **1997**, *101*, 4646–4652.
(38) Boys, S. F.; Bernardi, F. *Mol. Phys.* **1970**, *19*, 553–566.
(39) Slater, J. C. *The Self-consistent Field for Molecules and Solids*; McGraw-Hill: New York, 1974; Vol. 4.
(40) Vosko, S. H.; Wilk, L.; Nusair, M. *Can. J. Phys.* **1980**, *58*, 1200–1211.
(41) Becke, A. D. *J. Chem. Phys.* **1996**, *104*, 1040–1046.
(42) Lee, C.; Yang, W.; Parr, R. G. *Phys. Rev. B* **1988**, *37*, 785–789.
(43) Perdew, J. P. In *Electronic Structure of Solids '91*; Ziesche, P., Eschrig, H., Eds.; Akademie Vertag: Berlin, Germany, 1991; pp 11$-$20.
(44) Becke, A. D. *Phys. Rev. A* **1988**, *38*, 3098–3100.
(45) Adamo, C.; Barone, V. *J. Chem. Phys.* **1998**, *108*, 664–675.
(46) Lynch, B. J.; Zhao, Y.; Truhlar, D. G. *J. Phys. Chem. A* **2003**, *107*, 1384–1388.

(47) Staroverov, V. N.; Scuseria, G. E.; Tao, J.; Perdew, J. P. *J. Chem. Phys.* **2003**, *119*, 12129–12137.
(48) Zhao, Y.; Pu, J.; Lynch, B. J.; Truhlar, D. G. *Phys. Chem. Chem. Phys.* **2004**, *6*, 673–676.
(49) Boese, A. D.; Martin, J. M. L. *J. Chem. Phys.* **2004**, *121*, 3405–3416.
(50) Zhao, Y.; Schultz, N. E.; Truhlar, D. G. *J. Chem. Theory Comput.* **2006**, *2*, 364–382.
(51) Reed, A. E.; Weinhold, F. *J. Chem. Phys.* **1983**, *78*, 4066–4073.
(52) The tilt angle is a measure of the steric size of the cyclopentadienyl and phosphine ligands and is defined as the dihedral angle between the mean plane of the cyclopentadienyl carbons and the plane defined by the Os atom and the two phosphorus atoms. For any particular choice of the ancillary ligands, the tilt angle calculated for the methyl hydride complex **1** and its methane tautomer **2** were essentially identical.
(53) Stevenson, D. P.; Ibers, J. A. *J. Chem. Phys.* **1960**, *33*, 762–763.
(54) Becke, A. D. *J. Chem. Phys.* **1993**, *98*, 5648–5652.
(55) Dunning, T. H., Jr. *J. Chem. Phys.* **1989**, *90*, 1007–1023.
(56) Kendall, R. A.; Dunning, T. H., Jr.; Harrison, R. J. *J. Chem. Phys.* **1992**, *96*, 6796–6806.
(57) Woon, D. E.; Dunning, T. H., Jr. *J. Chem. Phys.* **1993**, *98*, 1358–1371.
(58) One conclusion of chemical importance is that changing the phosphine from the $(CH_3)_2PCH_2CH_2P(CH_3)_2$ ligand used experimentally to the model ligand $H_2PCH_2CH_2PH_2$ considerably lowers the energy of the methane tautomer relative to the methyl/hydride complex. This result is not surprising in view of the poorer donor ability of the model phosphine, which will reduce the back donation from the osmium center into the antibonding C−H orbital of the coordinated methane that is necessary to cleave the bond.
(59) Klein, R. A.; Zottola, M. A. *Chem. Phys. Lett.* **2006**, *419*, 254–258.
(60) Feller, D.; Peterson, K. A. *Chem. Phys. Lett.* **2006**, *430*, 459–463.
(61) Mattsson, A. *Science* **2002**, *298*, 759–760.
(62) Becke, A. D. *J. Chem. Phys.* **2000**, *112*, 4020–4026.
(63) Durant, J. L. *Chem. Phys. Lett.* **1996**, *256*, 595–602.
(64) Baker, J.; Andzelm, J.; Muir, M.; Taylor, P. R. *Chem. Phys. Lett.* **1995**, *237*, 53–60.
(65) Thakur, T. S.; Desiraju, G. R. *J. Mol. Struct.: THEOCHEM* **2007**, *810*, 143–154.
(66) Silva, V. D.; Dos Santos, E. N.; Gusevskaya, E. V.; Rocha, W. R. *J. Mol. Struct.: THEOCHEM* **2007**, *816*, 109–117.
(67) Khalimon, A. Y.; Lin, Z. H.; Simionescu, R.; Vyboishchikov, S. F.; Nikonov, G. I. *Angew. Chem.* **2007**, *119*, 4614–4617.
(68) Perdew, J. P.; Chevary, J. A.; Vosko, S. H.; Jackson, K. A.; Pederson, M. R.; Singh, D. J.; Fiolhais, C. *Phys. Rev. B* **1992**, *46*, 6671.
(69) Paier, J.; Marsman, M.; Kresse, G. *J. Chem. Phys.* **2007**, *127*, 024103/1–024103/10.
(70) Barone, V.; Biczysko, M.; Pavone, M. *Chem. Phys.* **2008**, *346*, 247–256.
(71) Zhao, Y.; Truhlar, D. G. *J. Chem. Theory Comput.* **2008**, *4*, 1849–1868.
(72) Hohenstein, E. G.; Chill, S. T.; Sherrill, C. D. *J. Chem. Theory Comput.* **2008**, *4*, 1996–2000.
(73) Grimme, S. *J. Comput. Chem.* **2004**, *25*, 1463–1473.
(74) Boehme, M.; Frenking, G. *Chem. Phys. Lett.* **1994**, *224*, 195–199.
(75) Olsen, J.; Christiansen, O.; Koch, H.; Jorgensen, P. *J. Chem. Phys.* **1996**, *105*, 5082–5090.

JP9058033